Albumin-mediated extracellular zinc speciation drives cellular zinc uptake

Received 00th January 20xx,
Accepted 00th January 20xx

DOI: 10.1039/x0xx00000x

James P. C. Coverdale,[a,b] Hugo A. van den Berg,[c] Siavash Khazaipoul,[d] Hannah E. Bridgewater,[a] Alan J. Stewart,[d] and Claudia. A. Blindauer*[a]

The role of the extracellular medium in influencing metal uptake into cells has not been described quantitatively. In a chemically-defined model system containing albumin, zinc influx into endothelial cells correlates with the extracellular free zinc concentration. Allosteric inhibition of zinc-binding to albumin by free fatty acids increased zinc flux.

Zinc is, after iron, the second-most abundant essential d-block metal in the body. Exclusively present in the 2+ oxidation state, Zn^{2+} is found in almost all cells, with total cytosolic concentrations in the hundreds of micromolar.[1] In mammals, Zn^{2+} is distributed throughout the body by blood plasma,[2] where total concentrations are around 10-23 µM Zn^{2+} under normal physiological conditions.[3] Transport from plasma into tissues requires Zn^{2+} uptake into cells, and although these total concentrations may suggest that zinc import occurs against a concentration gradient, this view is inappropriate, as it is the concentration of the "active" species – presumably the free Zn^{2+} ion or its simple small-molecule complexes – that needs to be considered.[4] Free metal concentrations are a consequence of binding affinities and concentrations of ligands in the respective solution, and here, the tables are turned, with non-protein bound Zn^{2+} estimated to lie in the (high) picomolar range in the cytosol,[1] and at least one order of magnitude higher in blood plasma.[5,6,7] Free Zn^{2+} above low nanomolar concentration is in fact remarkably toxic towards cells of all species including mammalian,[8] plant,[9] fungal and certain bacterial cells,[10] and so careful control of zinc homeostasis – also in the extracellular environment – is paramount to survival and health.

In mammals, serum albumin is the major carrier for Zn^{2+} in plasma.[11] Albumins from several species are known to bind Zn^{2+} at two principal binding sites: site A and site B.[12-16] Site A, sometimes also referred to as the 'multi-metal binding site',[13] is an interdomain site situated between domains I and II (**Fig. 1,** left).[15,16] X-ray crystallography of human (HSA) and equine serum albumins has shown that tetrahedral coordination of Zn^{2+} occurs between three amino acid residues (His67, His247 and Asp249) and a fourth solvent site.[15]

Owing to albumin's high concentration (>600 µM in human plasma), moderate affinity for Zn^{2+} (site A displays a low micromolar dissociation constant under physiological conditions),[17-20] and the labile fashion in which Zn^{2+} is bound, this site is responsible for the largest portion of the exchangeable plasma zinc pool. Thus, albumin – or more specifically site A – acts as the major determinant of zinc speciation in plasma.[8,21] Plasma zinc exchanges about 150 times

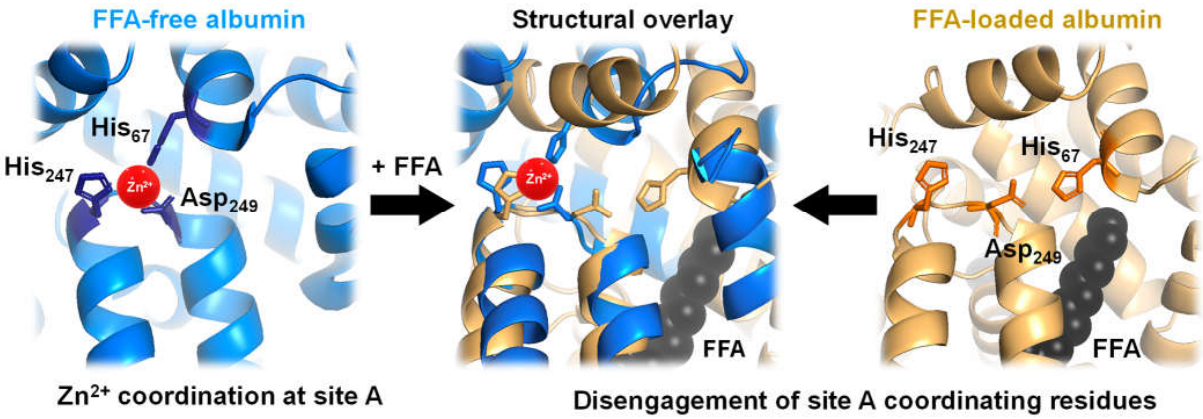

Fig. 1. Serum albumin is the principal Zn^{2+} transporter in the extracellular fluid. Amino acid residues His67, His247 and Asp249 form site A (green; PDB 5IJF; HSA), the interdomain principal binding site for Zn^{2+} (grey sphere). In the presence of FFAs of sufficient chain length bound at the nearby FFA binding site, FA2 (myristate C14:0 shown in blue), an allosteric mechanism is invoked, disengaging amino acid coordination at site A, as depicted in the structural overlay (centre). Upon disengagement of amino acid binding, Zn^{2+} affinity drops dramatically,[17,18] leading to release of Zn^{2+} from FFA-loaded albumin (pink; PDB 1BJ5; HSA[30]) under physiological conditions.[32]

[a] *Department of Chemistry, University of Warwick, Coventry, CV4 7AL, UK*
[b] *School of Pharmacy, Institute of Clinical Sciences, University of Birmingham, Edgbaston, B15 2TT, UK*
[c] *Warwick Mathematics Institute, University of Warwick, Coventry, CV4 7AL, UK*
[d] *School of Medicine, University of St. Andrews, St. Andrews, KY16 9TF, UK*

† Electronic Supplementary Information (ESI) available: Tables S1-S16, Figs. S1-S3, Materials and Methods, Derivation of Mathematical Model. See DOI: 10.1039/x0xx00000x

per day.[2] This illustrates starkly that zinc speciation in plasma is a highly dynamic process – not least because several processes occurring within plasma are zinc-mediated, including blood clotting, insulin activation, and immune function.[22-24] One particular group of metabolites has been shown to have a major impact on albumin-mediated zinc speciation: free (i.e., non-esterified) fatty acids (FFA). FFA levels in plasma are also highly dynamic, and are significantly elevated under certain physiological (e.g. fasting) and pathological (diabetes, obesity) conditions.[25,26] Although several fatty acid binding sites have been identified in crystallographic and NMR spectroscopic studies of albumin,[27,28] the high-affinity FA2 site (**Fig. 1**, right) is of particular interest in relation to zinc speciation. Binding of FFAs to FA2 elicits a considerable structural change to the domain I/II interface, with His67 (domain I) being displaced from the vicinity of His247 and Asp249 (domain II) (**Fig. 1**, centre). This interaction depends on the nature of the FFA, including its length, whereby only medium-to-long chain fatty acids (>C12) cause the allosteric switch.[29,30] Isothermal titration calorimetry of bovine serum albumin (BSA) and HSA has demonstrated that this dramatically decreases their Zn^{2+}-binding capacity.[14,17,25,29,31] We recently quantified changes in Zn^{2+} speciation in bovine serum and human plasma resulting from elevated free fatty acid (FFA) concentrations, and found that a re-distribution of Zn^{2+} from albumin (BSA or HSA) to other proteins occurs.[32] More recently, we have shown that FFAs affect zinc-mediated processes such as platelet aggregation and fibrin clotting via albumin.[29] Both processes depend on the concentration of Zn^{2+} that is available to bind to the proteins involved.

The present study is based on the hypothesis that previously observed effects of albumin-mediated zinc speciation on cells[8] are due to more "free" Zn^{2+} becoming available to membrane-bound transporters such as ZIPs,[33] which would result in increased zinc uptake. We test this hypothesis by quantitatively assessing Zn^{2+} influx (φ_{in}) and efflux (φ_{out}) rates in model systems with well-defined concentrations of bovine serum albumin (BSA) and Zn^{2+}. Moreover, we assess the effect of FFAs (octanoate, myristate and palmitate) on flux rates, and whether this affects zinc toxicity.

Zinc binding in both BSA and HSA are affected similarly by FFA binding,[31] so BSA may serve as an appropriate model for mammalian albumins. Furthermore, the widespread use of foetal bovine serum in media for culturing human cell lines highlights the relevance of BSA-based model systems. Indeed, the importance of zinc buffering and speciation in cell culture media in general,[34] and by albumin in particular[8,35] has been demonstrated in recent years.

We selected a human umbilical vascular endothelial cell (HUVEC) model, as *in vivo*, vascular endothelial cells are in direct contact with blood plasma and form a barrier through which all nutrients, including Zn^{2+}, must pass prior to entry into peripheral tissues. Endothelial cell models thus provide a well-defined system that is pertinent for assessing the role(s) that albumin plays in cellular zinc uptake. Primary HUVECs were immortalised using human telomerase reverse transcriptase (hTERT) to provide a homologous cell line for further study (**ESI† Materials and Methods**). The resultant cells exhibited a typical endothelial cell morphology in culture and retain expression of HUVEC markers including CD31, von Willebrand factor, and VE-cadherin (**ESI† Fig. S1**).

For the determination of zinc flux rates, we developed a stable isotope approach. Traditionally, zinc dynamics have often been assessed using radioactive ^{65}Zn. This comes with several drawbacks, including the fact that ^{65}Zn decays to ^{65}Cu, which introduces another chemical element that may affect cells. A recent study highlighted the merits of working with stable isotopes.[36]

Before commencement of the isotope assay, immortalised HUVECs were first equilibrated to physiologically relevant conditions (600 µM BSA and 20 µM natural-abundance Zn^{2+} (designated as "pre-conditioning medium", **Fig. 2**) for 24 h. After this time, cells were washed with phosphate-buffered saline and incubated in fresh medium containing 20 µM $^{68}Zn^{2+}$ (>99% ^{68}Zn; **ESI† Table S1**) with different extracellular BSA concentrations (0-600 µM). Cell pellets were collected at defined time intervals, digested with ultrapure concentrated nitric acid, and the intracellular isotopic ratio $^{66}Zn/^{68}Zn$ was measured by standard inductively-coupled plasma-mass spectrometry (ICP-MS) (**Fig. 2(a)**). Additionally, the total amount of intracellular Zn^{2+} (Q_0 and $Q(t)$) was determined from the sum of all zinc isotopes (**Fig. 2(b)**).

For cells treated with 60-600 µM BSA, the total intracellular [Zn] remained constant (~50 ng per million cells: **Fig. 2(b)** and **ESI† Tables S2** and **S3**). This indicates that the cells are able to control their total contents, and that rates of influx (φ_{in}) and efflux (φ_{out}) are equal, $\varphi_{in} = \varphi_{out}$. In contrast, cells in the presence of lower concentrations of BSA (0 and 40 µM) accumulated zinc over time (**Fig. 2(b)** and **ESI† Tables S2** and

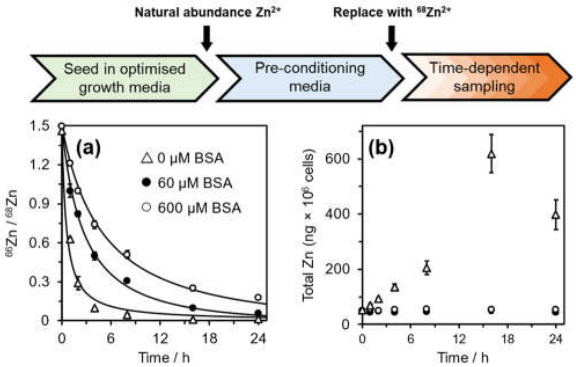

Fig. 2. $^{66}Zn/^{68}Zn$ ratios determined at different extracellular [albumin] concentrations (0-600 µM; see **ESI†** for full data). Phase I: cells seeded and allowed to proliferate to full confluence in HUVEC cell culture medium; Phase II: cells are cultured in physiologically relevant media containing 600 µM BSA + 20 µM natural abundance Zn^{2+} without additional FFA; Phase III: cells are washed with PBS, and extracellular medium is replaced with fresh medium containing variable concentrations of BSA (0-600 µM) + 20 µM isotopically-enriched $^{68}Zn^{2+}$. Cell pellets were collected in a time-dependent manner and analysed by ICP-MS (He-gas mode) after whole-cell acidic digestion. **(a)** $^{66}Zn/^{68}Zn$ ratios were calculated, plotted and fitted to a mathematical model to derive zinc flux rates. Zinc flux increases with decreasing BSA concentration. **(b)** Zinc isotopes (^{64}Zn, ^{66}Zn, ^{67}Zn, ^{68}Zn, ^{70}Zn) were summed up to determine total intracellular zinc (ng × 10^6 cells). For extracellular BSA > 60 µM, intracellular [Zn] remained constant at ca. 50 ng × 10^6 cells but increased for extracellular BSA < 40 µM. See ESI† Tables S2-S5 and S9-S13 for full numerical data and mathematical models.

S3), *i.e.,* influx rates are larger than efflux rates; $\varphi_{in} > \varphi_{out}$.

We sought to derive quantitative information on zinc fluxes from these data, and developed a mathematical model to describe the $^{66}Zn/^{68}Zn$ ratio as a function of time:

$$\frac{^{66}Zn}{^{68}Zn}(t) = \frac{r_{66,ex} - (r_{66,ex} - \tilde{r}_{66})G(t)}{r_{68,ex} - (r_{68,ex} - \tilde{r}_{68})G(t)} \quad (1)$$

where $r_{66,ex}$ (or $r_{68,ex}$) is the relative abundance of ^{66}Zn (or ^{68}Zn) in the incubation medium, $\tilde{r}_{66}$ or $\tilde{r}_{68}$ is the natural relative abundance of ^{66}Zn or ^{68}Zn, and $G(t)$ is a function given by

$$G(t) = \left(1 + \frac{(\varphi_{in} - \varphi_{out})}{Q(t_0)}(t - t_0)\right)^{-\varphi_{in}/(\varphi_{in} - \varphi_{out})} \quad (2)$$

where t_0 denotes the point in time at which the experiment is started, $Q(t_0)$ the total cellular zinc content at time $t = t_0$, φ_{in} the influx, and φ_{out} the efflux of zinc. This relationship is based on the assumption that both fluxes are constant for the duration of the experiment (see **ESI†** for validation). In cases where cells do not accumulate zinc over time ($Q(t) \equiv Q_0$, and hence $\varphi_{in} = \varphi_{out} \equiv \varphi$), $G(t)$ reduces to

$$G(t) = \exp\{-(\varphi/Q_0)(t - t_0)\}. \quad (3)$$

The datasets for 60, 160 and 600 μM BSA were treated using the latter relationship; those at 0 and 40 μM BSA used equation (2). Representative fits are shown in **Fig. 2**, all fitting results are collected in **ESI†, Fig. S2** and **Tables S4, S5** and **S9-S13**. The zinc influx rates obtained (2.51-22.82 fg·h^{-1}·cell^{-1}) are comparable to those found in previous studies. An early radio-chemical study determined $^{65}Zn^{2+}$ influx rates into human and rat erythrocytes of 0.22 fg·h^{-1}·cell^{-1},[37] while an ICP-MS study of $^{70}Zn^{2+}$ influx into human HEK293T cells in the presence of Zn-depleted media determined rates of 23.5 fg·h^{-1}·cell^{-1}.[36]

Plotting the influx rates vs total [BSA] clearly shows that cellular zinc uptake rates are dependent on albumin concentration (**Fig. 3(a)**). This can be rationalised on the basis that BSA controls zinc speciation, and that free [Zn^{2+}] governs interaction with membrane-bound zinc transporters – and hence transport. This is clearly seen in **Fig. 3(b)**, where we have estimated free [Zn^{2+}], based on published stability constants for site A,[19,31] and replotted the observed influx rates *vs.* these. This plot suggests that in this low concentration range, transport kinetics are 1st order in free [Zn^{2+}], in agreement with expectations for transport of single species across membranes[38] and previous findings in hepatocytes.[39] This correlation is also compatible with kinetic data for a bacterial ZIP protein.[40]

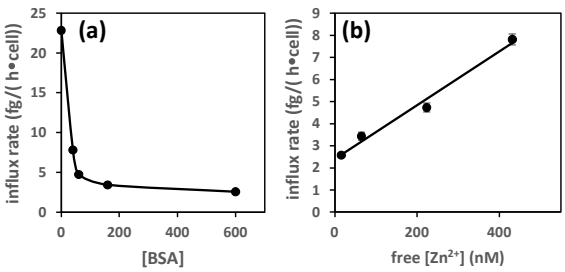

Fig. 3. Zinc influx depends on the concentration of albumin (a). This can be correlated to free [Zn] for [BSA] = 40-600 μM (estimated using published stability constants for site A only; see **ESI†**) (b) In this range the influx rate shows a linear relationship with free [Zn^{2+}].

Having thus found that, in systems where BSA is the only significant zinc buffer, this protein governs zinc uptake rates via regulating free [Zn^{2+}], we explored next the impact of FFAs on zinc uptake. Previous work has shown that 5 molar equivalents of long-chain FFAs (levels that can be encountered in certain (patho)physiological conditions)[28] had a pronounced effect on site A availability.[17,29,31] For these experiments, we chose a BSA concentration of 60 μM, for several reasons: (i) at 60 μM fatty-acid free BSA, cellular zinc contents remained stable, (ii) a solution that contains 10% of physiological levels is reminiscent of cell culture media, and (iii) long-chain FFAs are sparingly soluble in neutral aqueous solutions, so achieving concentrations that would be high enough to match those required for 600 μM BSA is experimentally challenging. Thus, the medium for time-dependent sampling contained 60 μM BSA, 20 μM Zn^{2+}, and was supplemented with 300 μM octanoate (C8:0), myristate (C14:0), or palmitate (C16:0).

Addition of myristate or palmitate significantly increased the rate of intracellular ^{68}Zn isotope enrichment, whilst octanoate had no discernible effect (**Fig. 4, ESI† Table S5** and **S7**). Furthermore, the increased change in the $^{66}Zn/^{68}Zn$ ratio observed in the presence of myristate or palmitate was accompanied by a gradual increase in total intracellular zinc over time, indicating that cells were no longer able to balance influx and efflux (**ESI† Tables S3** and **S6**). Accordingly, fitting the data to our model (equation 2) gave φ_{iin} = 7.45 ± 0.34 in the presence of myristate or 7.99 ± 0.24 fg·h^{-1}·cell^{-1} in the presence of palmitate, compared to 4.73 ± 0.20 fg·h^{-1}·cell^{-1} in the absence of FFA. In contrast, the rate for BSA treated with octanoate (5.03 ± 0.31 fg·h^{-1}·cell^{-1}) remained statistically unchanged relative to the FFA-free experiment (**Fig. 4, ESI† Table S5**). These observations agree with earlier chromatographic, NMR and ITC studies, which suggest that octanoate is too short to activate the allosteric switch.[17,29,31,32]

Finally, to test whether zinc speciation and the resulting increased influx affects zinc toxicity, we determined IC_{50} values in cells grown at different [BSA] (**ESI† Table S8** and **Fig. S3**). At 600 μM BSA, an IC_{50} value of 1025 ± 12 μM Zn^{2+} was found, contrasting with 11.80 ± 0.05 μM in the absence of BSA. The increased influx observed in presence of long-chain FFAs was also accompanied by increased toxicity, with IC_{50} dropping from 111 ± 2 μM to 66.7 ± 0.9 μM for experiments at 60 μM BSA in the absence and presence of myristate, respectively. These results indicate that increased influx is accompanied by measurable effects on cells.

In summary, we have developed an integrated quantitative approach that permits the determination of zinc flux rates in (endothelial) cells. Supplying a single stable isotope in the extracellular medium, monitoring isotopic ratios over time, and mathematical modelling allows assessing zinc uptake under essentially physiological conditions. Crucially, our approach does neither require the cells to accumulate more zinc than their physiological quota, nor the administration of any additional reagents.

Our findings provide the first directly quantifiable evidence

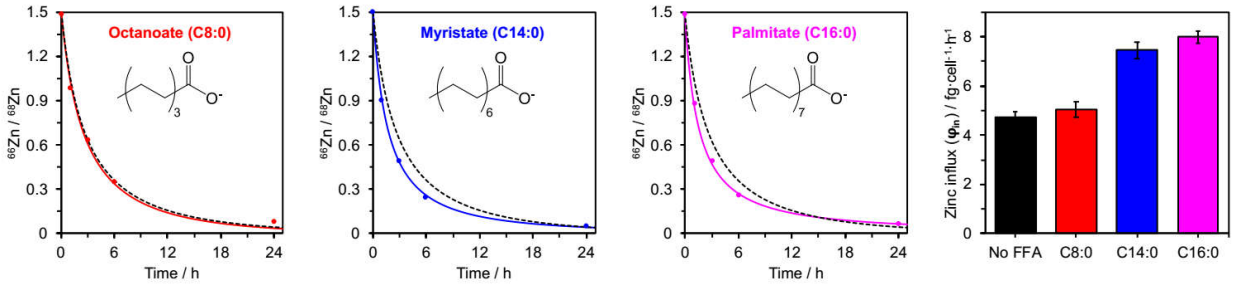

Fig. 4. Isotopic ratios (^{66}Zn / ^{68}Zn) over time for HUVEC cells cultured in presence of 60 μM BSA and either C8:0 (octanoate), C14:0 (myristate) or C16:0 (palmitate) FFAs (300 μM, 5 mol. equiv.). Experimental data (•) are shown with corresponding fitting model for that experimental condition (**solid coloured line**) alongside the fitting model for 60 μM BSA in the absence of FFAs (**dashed black line**). The right-hand panel compares the influx rates φ_{in} for these four conditions. Full numerical data can be found in **ESI†, Tables S6, S7** and **S14-S16**.

that (i) extracellular zinc speciation governs zinc uptake rates, and (ii) FFAs may affect cellular zinc uptake, via the allosteric switch on albumin. This may imply that *in vivo* acute and chronic elevations of plasma FFAs drive increased export of Zn^{2+} from plasma. We note however that at physiological albumin concentrations (*ca*. 600 μM), total cellular zinc contents would not be expected to increase like for [BSA] = 60 μM. Future efforts should evaluate zinc flux rates in more complex, multi-protein systems, and may involve refinements of isotope measurements and mathematical models.

This work was financially supported by the Leverhulme Trust (RPG-2017-214) and BBSRC (BB/J006467/1 and BB/V014684/1). We thank Prof. Andrew Riches (University of St. Andrews) for provision of materials, and Dr. Elizabeth Bolitho (University of Warwick) for assistance with cell culture experiments.

Conflicts of interest

There are no conflicts to declare.

Notes and references

1. A. Krezel and W. Maret, *J. Biol. Inorg. Chem.*, 2006, **11**, 1049-1062.
2. J. C. King, *Am. J. Clin. Nutr.*, 2011, **94**, 679s-684s.
3. M. Rükgauer, J. Klein and J. D. Kruse-Jarres, *J. Trace Elem. Med. Biol.*, 1997, **11**, 92-98.
4. A. W. Foster, D. Osman and N. J. Robinson, *J. Biol. Chem.*, 2014, **289**, 28095-28103.
5. J. W. Foote and H. T. Delves, *Analyst*, 1988, **109**, 709-711.
6. W. Alker, T. Schwerdtle, L. Schomburg and H. Haase, *Int. J. Mol. Sci.*, 2019, **20**, 4006.
7. P. Zalewski, A. Truong-Tran, S. Lincoln, D. Ward, A. Shankar, P. Coyle, L. Jayaram, A. Copley, D. Grosser, C. Murgia, C. Lang and R. Ruffin, *BioTechniques*, 2006, **40**, 509-520.
8. H. Haase, S. Hebel, G. Engelhardt and L. Rink, *Metallomics*, 2015, **7**, 102-111.
9. G. R. Rout and P. Das, in *Sustainable Agriculture*, eds. E. Lichtfouse, M. Navarrete, P. Debaeke, S. Véronique and C. Alberola, Springer Netherlands, Dordrecht, 2009, DOI: 10.1007/978-90-481-2666-8_53, pp. 873-884.
10. H. Babich and G. Stotzky, *Appl. Environ. Microbiol.*, 1978, **36**, 906-914.
11. C. A. Blindauer, I. Harvey, K. E. Bunyan, A. J. Stewart, D. Sleep, D. J. Harrison, S. Berezenko and P. J. Sadler, *J. Biol. Chem.*, 2009, **284**, 23116-23124.
12. J. Lu, A. J. Stewart, P. J. Sadler, T. J. Pinheiro and C. A. Blindauer, *Biochem Soc Trans*, 2008, **36**, 1317-1321.
13. W. Bal, J. Christodoulou, P. J. Sadler and A. Tucker, *J. Inorg. Biochem.*, 1998, **70**, 33-39.
14. J. P. Barnett, C. A. Blindauer, O. Kassaar, S. Khazaipoul, E. M. Martin, P. J. Sadler and A. J. Stewart, *Biochim. Biophys. Acta, Gen. Subj.*, 2013, **1830**, 5456-5464.
15. K. B. Handing, I. G. Shabalin, O. Kassaar, S. Khazaipoul, C. A. Blindauer, A. J. Stewart, M. Chruszcz and W. Minor, *Chem. Sci.*, 2016, **7**, 6635-6648.
16. A. J. Stewart, C. A. Blindauer, S. Berezenko, D. Sleep and P. J. Sadler, *Proc. Natl. Acad. Sci. U.S.A.*, 2003, **100**, 3701-3706.
17. O. Kassaar, U. Schwarz-Linek, C. A. Blindauer and A. J. Stewart, *J. Thromb. Haemost.*, 2015, **13**, 101-110.
18. J. Lu, A. J. Stewart, D. Sleep, P. J. Sadler, T. J. T. Pinheiro and C. A. Blindauer, *J. Am. Chem. Soc.*, 2012, **134**, 1454-1457.
19. E. Ohyoshi, Y. Hamada, K. Nakata and S. Kohata, *J. Inorg. Biochem.*, 1999, **75**, 213-218.
20. J. Masuoka and P. Saltman, *J. Biol. Chem.*, 1994, **269**, 25557-25561.
21. J. P. C. Coverdale, S. Khazaipoul, S. Arya, A. J. Stewart and C. A. Blindauer, *Biochim. Biophys. Acta Mol. Cell Biol. Lipids*, 2019, **1864**, 532-542.
22. S. J. Hierons, J. S. Marsh, D. Wu, C. A. Blindauer and A. J. Stewart, *Int. J. Mol. Sci.*, 2021, **22**.
23. S. Arya, A. J. Gourley, J. C. Penedo, C. A. Blindauer and A. J. Stewart, *BioEssays*, 2021, **43**, e2100172.
24. I. Wessels, M. Maywald and L. Rink, *Nutrients*, 2017, **9**, 1286.
25. C. A. Blindauer, S. Khazaipoul, R. Yu and A. J. Stewart, *Curr. Topics Med. Chem.*, 2016, **16**, 3021-3032.
26. J. P. C. Coverdale, K. G. H. Katundu, A. I. S. Sobczak, S. Arya, C. A. Blindauer and A. J. Stewart, *Prostaglandins, Leukotrienes Essent. Fatty Acids*, 2018, **135**, 147-157.
27. S. Curry, P. Brick and N. P. Franks, *Biochim. Biophys. Acta - Mol. Cell Biol. Lipids*, 1999, **1441**, 131-140.
28. J. R. Simard, P. A. Zunszain, C. E. Ha, J. S. Yang, N. V. Bhagavan, I. Petitpas, S. Curry and J. A. Hamilton, *Proc. Natl. Acad. Sci. U. S. A.*, 2005, **102**, 17958-17963.
29. A. I. S. Sobczak, K. G. H. Katundu, F. A. Phoenix, S. Khazaipoul, R. Yu, F. Lampiao, F. Stefanowicz, C. A. Blindauer, S. J. Pitt, T. K. Smith, R. A. Ajjan and A. J. Stewart, *Chem. Sci.*, 2021, **12**, 4079-4093.
30. S. Curry, H. Mandelkow, P. Brick and N. Franks, *Nature Struct. Biol.*, 1998, **5**, 827-835.
31. J. Lu, A. J. Stewart, P. J. Sadler, T. J. T. Pinheiro and C. A. Blindauer, *J. Med. Chem.*, 2012, **55**, 4425-4430.
32. J. P. C. Coverdale, J. P. Barnett, A. H. Adamu, E. J. Griffiths, A. J. Stewart and C. A. Blindauer, *Metallomics*, 2019, **11**, 1805-1819.
33. T. Kambe, T. Tsuji, A. Hashimoto and N. Itsumura, *Physiol. Rev.*, 2015, **95**, 749-784.
34. W. Maret, *Metallomics*, 2015, **7**, 202-211.
35. M. Maares, A. Duman, C. Keil, T. Schwerdtle and H. Haase, *Metallomics*, 2018, **10**, 979-991.
36. C. E. R. Richardson, E. M. Nolan, M. D. Shoulders and S. J. Lippard, *Biochemistry*, 2018, **57**, 6807-6815.
37. N. M. Horn, A. L. Thomas and J. D. Tompkins, *J. Phys.*, 1995, **489**, 73-80.
38. B. Alberts, J. A., J. Lewis, M. Raff, K. Roberts and P. Walter, *Molecular Biology of the Cell, 4th Edition*, Garland Science, New York, 2002.
39. J. A. Taylor and T. J. Simons, *J Physiol*, 1994, **474**, 55-64.
40. W. Lin, J. Chai, J. Love and D. Fu, *J Biol Chem*, 2010, **285**, 39013-39020.

Fatty acids modulate zinc uptake into cells via albumin binding

James P. C. Coverdale, Hugo A. van den Berg, Siavash Khazaipoul, Hannah E. Bridgewater, Alan J. Stewart, and Claudia. A. Blindauer

Supplementary Information

Supplemental Tables S1-S16

Supplemental Figures S1-S3

Materials and Methods

Derivation of the Mathematical Model

Table S1. Isotopic purity of ^{68}Zn stock solutions (500 µM in 1× HEPES-buffered EBSS), determined by ICP-MS in He-gas mode. These isotopic abundances were considered in mathematical modelling of experimental data.

Analyte	Abundance (%)
^{64}Zn	0.08
^{66}Zn	0.05
^{67}Zn	0.33
^{68}Zn	99.33
^{70}Zn	0.21

Table S2. Total intracellular Zn (fg·cell^{-1}) determined for the intracellular Zn concentration in immortalised HUVEC cells treated with isotopically enriched $^{68}Zn^{2+}$ (20 μM solution in EBSS, pH 7.4) for defined time period (*t*) with defined supplementation using bovine serum albumin (BSA; 0-0.6 mM), after 24 h pre-incubation under physiological conditions (20 μM natural abundance Zn^{2+}, 0.6 mM BSA solution in EBSS, pH 7.4).

Total intracellular Zn (fg·cell^{-1})					
Time / h	**0 μM BSA**	**40 μM BSA**	**60 μM BSA**	**160 μM BSA**	**600 μM BSA**
0	52 ± 4	52 ± 2	50 ± 1	52 ± 2	50 ± 2
0.08 (5 min)	54 ± 4	-	-	-	-
0.17 (10 min)	56 ± 2	-	-	-	-
0.33 (20 min)	55.9 ± 0.5	-	-	-	-
0.5 (30 min)	60 ± 9	-	-	-	-
0.67 (40 min)	60± 4	-	-	-	-
0.83 (50 min)	61 ± 5	-	-	-	-
1	68 ± 7	64 ± 3	45 ± 3	55 ± 1	56 ± 3
2	93 ± 2	-	48 ± 1	-	50 ± 4
3	-	70 ± 4	-	50 ± 6	-
4	135 ± 11	-	44 ± 5	-	54 ± 3
6	-	81 ± 5	-	48 ± 2	-
8	205 ± 25	-	46 ± 3	-	56 ± 5
16	619 ± 69	-	52 ± 12	-	54 ± 6
24	398 ± 54	110 ± 12	45 ± 8	53 ± 5	53 ± 2

Table S3. P-values testing whether immortalised HUVEC cells significantly accumulate zinc, using linear regression alongside calculated slopes (fg·cell^{-1}·h^{-1}) and calculated standard error. Probabilities shown relate to experimental data reported in either **Table S2** (variable bovine serum albumin concentration 0-600 μM, no FFA) or **Table S5** (FFAs supplemented at 300 μM, 5 mol. equiv., with BSA concentration fixed at 60 μM).

BSA / μM	FFA	Slope / fg·cell^{-1}·h^{-1} (standard error)	P-value
0	-	20.4266 (3.27769)	0.000065
40	-	2.14023 (0.351819)	0.0089
60	-	0.00854449 (0.14761)	0.96
60	C8:0 (5 mol. equiv.)	0.0117707 (0.0312627)	0.73
60	C14:0 (5 mol. equiv.)	1.31218 (0.226061)	0.010
60	C16:0 (5 mol. equiv.)	1.45548 (0.262727)	0.012
160	-	0.0271238 (0.157038)	0.87
600	-	0.0521509 (0.122045)	0.69

Table S4. Isotopic ratios ($^{66}Zn/^{68}Zn$) determined for the intracellular Zn concentration in immortalised HUVEC cells treated with isotopically enriched $^{68}Zn^{2+}$ (20 µM solution in EBSS, pH 7.4) for defined time period (*t*) with defined supplementation using BSA (0-0.6 mM), after 24 h pre-incubation under physiological conditions (20 µM natural abundance Zn^{2+}, 0.6 mM BSA solution in EBSS, pH 7.4).

Intracellular Zn isotopic ratio ($^{66}Zn/^{68}Zn$)					
Time / h	**0 µM BSA**	**40 µM BSA**	**60 µM BSA**	**160 µM BSA**	**600 µM BSA**
0	1.462 ± 0.009	1.514 ± 0.003	1.501 ± 0.005	1.514 ± 0.003	1.495 ± 0.006
0.08 (5 min)	1.39 ± 0.02	-	-	-	-
0.17 (10 min)	1.29 ± 0.03	-	-	-	-
0.33 (20 min)	1.20 ± 0.02	-	-	-	-
0.5 (30 min)	1.05 ± 0.02	-	-	-	-
0.67 (40 min)	1.0 ± 0.2	-	-	-	-
0.83 (50 min)	0.771 ± 0.008	-	-	-	-
1	0.63 ± 0.01	0.89 ± 0.04	1.00 ± 0.05	1.1 ± 0.2	1.21 ± 0.02
2	0.29 ± 0.05	-	0.82 ± 0.02	-	1.00 ± 0.02
3	-	0.47 ± 0.02	-	0.8 ± 0.1	-
4	0.097 ± 0.003	-	0.50 ± 0.03	-	0.74 ± 0.03
6	-	0.27 ± 0.01	-	0.47 ± 0.06	-
8	0.047 ± 0.006	-	0.308 ± 0.003	-	0.51 ± 0.03
16	0.011 ± 0.002	-	0.099 ± 0.003	-	0.25 ± 0.02
24	0.012 ± 0.002	0.046 ± 0.003	0.059 ± 0.006	0.105 ± 0.002	0.18 ± 0.01

Table S5. Mathematical modelling estimates for zinc flux rates (Φ_{in} and Φ_{out}, fg·cell^{-1}·h^{-1}) as a function of extracellular [BSA] and supplementation of free fatty acids (FFAs). The total intracellular zinc concentration ($Q(t)$)(**ESI† Tables S2, S3** and **S5**) dictated the modelling approach.[a,b]

			Zinc flux (fg·cell^{-1}·h^{-1})	
[BSA] (μM)	**FFA**	**Constant $Q(t)$?**	φ_{in}	φ_{out}
0	-	No	22.82 ± 2.61	2.39 [c]
40	-	No	7.81 ± 0.25	3.54 ± 0.86
60	-	Yes	4.73 ± 0.20	4.73 ± 0.20
160	-	Yes	3.43 ± 0.18	3.43 ± 0.18
600	-	Yes	2.57 ± 0.09	2.57 ± 0.09
60	C8:0	Yes	5.03 ± 0.31	5.03 ± 0.31
60	C14:0	No	7.45 ± 0.34	4.64 ± 0.78
60	C16:0	No	7.99 ± 0.24	2.51 ± 1.22

[a] Uncertainties in columns 4 and 5 refer to standard errors.

[b] Comparison across all data sets (except [BSA] = 0 μM) showed that the variation of φ_{in} was highly significant ($F\{2,29\} = 4.26$, $P = 1.15 \cdot 10^{-16}$) whereas the variation of φ_{out} was not significant at the 1% level ($F\{2,29\} = 4.26$, $P = 0.024$).

[c] $\varphi_{in} - \varphi_{out}$ was constrained by the slope of accumulation (20.43) (**ESI† Table S3**)

Table S6. Total intracellular Zn (fg·cell^{-1}) determined for the intracellular Zn concentration in immortalised HUVEC cells treated with isotopically enriched $^{68}Zn^{2+}$ (20 μM) for defined time period (*t*) with defined supplementation using BSA (60 μM) + 5 mol. equiv. FFA (octanoate, myristate, or palmitate), after 24 h pre-incubation under physiological conditions (20 μM natural abundance Zn^{2+}, 600 μM BSA solution in EBSS, pH 7.4).

Total intracellular Zn (fg·cell^{-1})			
Time (t) / h	**Octanoate (C8:0)**	**Myristate (C14:0)**	**Palmitate (C16:0)**
0	50 ± 6	55 ± 6	52 ± 9
1	50 ± 5	61 ± 4	56 ± 14
3	49 ± 5	61 ± 6	64 ± 8
6	49 ± 3	73 ± 9	72 ± 5
24	50 ± 2	89 ± 7	90 ± 18

Table S7. Isotopic ratios ($^{66}Zn/^{68}Zn$) determined for the intracellular Zn concentration in immortalised HUVEC cells treated with isotopically enriched $^{68}Zn^{2+}$ (20 μM) for defined time period (*t*) with defined supplementation using BSA(60 μM) + 5 mol. equiv. FFA (octanoate, myristate, or palmitate), after 24 h pre-incubation under physiological conditions (20 μM natural abundance Zn^{2+}, 600 μM BSA BSA solution in EBSS, pH 7.4).

Intracellular Zn isotopic ratio ($^{66}Zn/^{68}Zn$)			
Time (t) / h	**Octanoate (C8:0)**	**Myristate (C14:0)**	**Palmitate (C16:0)**
0	1.480 ± 0.006	1.503 ± 0.005	1.480 ± 0.006
1	0.98 ± 0.04	0.90 ± 0.02	0.88 ± 0.03
3	0.63 ± 0.04	0.49 ± 0.01	0.49 ± 0.01
6	0.35 ± 0.02	0.2442 ± 0.0002	0.259 ± 0.002
24	0.080 ± 0.002	0.047 ± 0.001	0.064 ± 0.008

Table S8. IC_{50} concentrations for Zn^{2+} (administered as $ZnCl_2$) determined in immortalised HUVEC cells in the presence of BSA (0-600 μM) with defined supplementation with free fatty acids (FFAs): either none, C8:0 (as sodium octanoate), or C14:0 (as sodium myristate). P-values for the latter two conditions refer to the comparison to the fatty acid-free control at 60 μM BSA and were calculated using a two-tailed *t*-test assuming unequal variances (Welch's *t*-test). Data are shown graphically in **Figure S3**.[a)]

BSA / μM	FFA	IC_{50} / μM
0	-	11.80 ± 0.05
6	-	17.4 ± 0.1
30	-	50.4 ± 0.4
60	-	111 ± 2
60	C8:0 (300 μM, 5 mol. equiv.)	108 ± 3 (p=0.2452)
60	C14:0 (300 μM, 5 mol. equiv.)	66.7 ± 0.9 (p=0.0008) ***
600	-	1025 ± 12

[a)] Using the datapoints at 0, 30, 60 and 600 μM BSA, assuming that in all cases, free $[Zn^{2+}]$ = 11.80 μM (corresponding to the IC_{50} for free $[Zn^{2+}]$, and with the approximations that (i) at excess zinc, site A is fully occupied, and (ii) the remainder of binding is due to site B, it is possible to estimate the conditional stability constant for site B as log K' = 5.0±0.4.

Tables S9-S16. Mathematical modelling results (data fits shown in Figure S3). Note that in cases where only the parameter ϕ_{in} is given, ϕ_{out} is equal to ϕ_{in}, as no change in total intracellular Zn (Q) occurred.

Table S9: 0 μM BSA*				
	Estimate	**Standard Error**	**t-Statistic**	**P-value**
ϕ_{in}	20.4266	3.27769	6.232	0.0000642045
ϕ_{out}	2.39 *	-	-	-

Table S10: 40 μM BSA				
	Estimate	**Standard Error**	**t-Statistic**	**P-value**
ϕ_{in}	7.81046	0.245476	31.8176	0.000068
ϕ_{out}	3.53528	0.855783	4.13105	0.026

Table S11: 60 μM BSA				
	Estimate	**Standard Error**	**t-Statistic**	**P-value**
ϕ_{in}	4.73129	0.199874	23.6713	3.73×10^{-7}

Table S12: 160 μM BSA				
	Estimate	**Standard Error**	**t-Statistic**	**P-value**
ϕ_{in}	3.43565	0.18388	18.6843	0.000048

Table S13: 600 μM BSA				
	Estimate	**Standard Error**	**t-Statistic**	**P-value**
ϕ_{in}	2.56974	0.0906118	28.3599	1.27×10^{-7}

Table S14: 60 μM BSA + sodium octanoate (C8:0, 0.3 mM, 5 mol. equiv.)				
Table S13	**Estimate**	**Standard Error**	**t-Statistic**	**P-value**
ϕ_{in}	5.03793	0.30771	16.3723	0.000081

Table S15: 60 μM BSA + sodium myristate (C14:0, 0.3 mM, 5 mol. equiv.)				
	Estimate	**Standard Error**	**t-Statistic**	**P-value**
ϕ_{in}	7.4492	0.230988	32.2493	0.000066
ϕ_{out}	4.6454	0.775272	5.99196	0.0093

Table S16: 60 μM BSA + sodium palmitate (C16:0, 0.3 mM, 5 mol. equiv.)				
	Estimate	**Standard Error**	**t-Statistic**	**P-value**
ϕ_{in}	7.98621	0.336722	23.7175	0.00016
ϕ_{out}	2.50888	1.21877	2.05853	0.13

* ϕ_{out} estimated from difference between slope (Table S3) and ϕ_{in}.

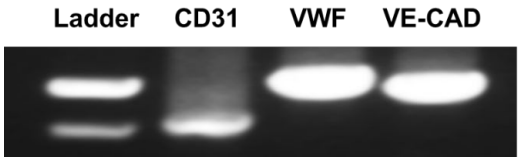

Figure S1. mRNA expression of endothelial marker proteins in immortalised HUVECs; CD31, von Willebrand factor (vWF) and VE-cadherin (VE-CAD).

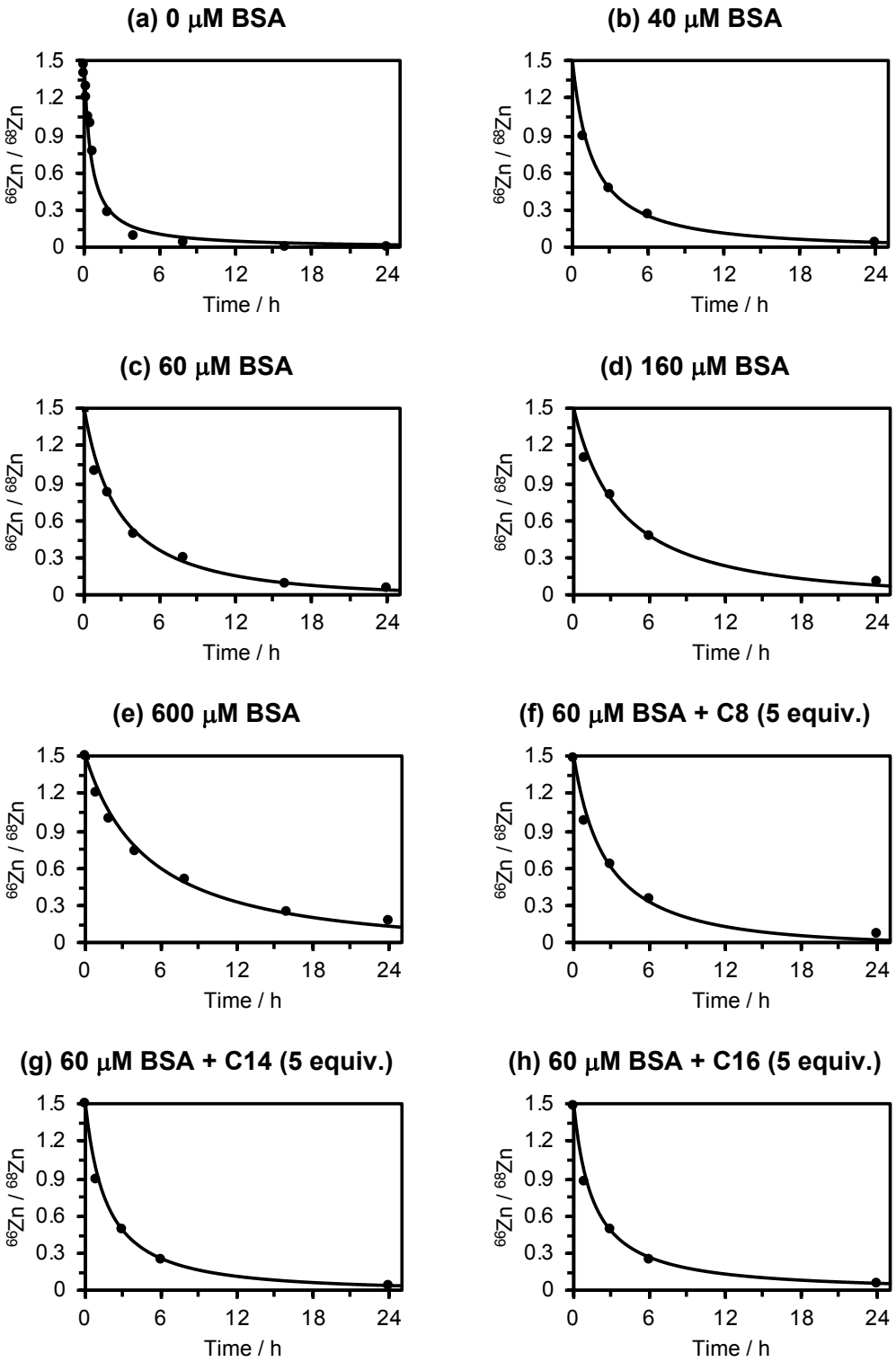

Figure S2. (a-h) Mathematical model fitting (curves) overlaid with experimental data (•) for the determined $^{66}Zn/^{68}Zn$ ratio over time in immortalised HUVECs. Fitting parameters and statistics: **Tables S8-S15**. Experimental data: **Tables S4** and **S6**.

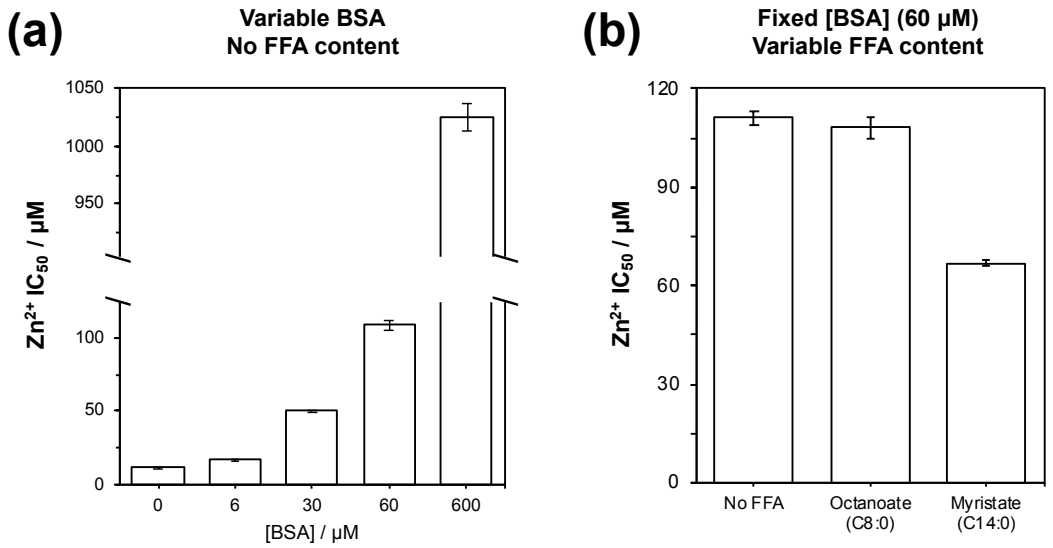

Figure S3. Zinc toxicity (IC_{50} / µM) determined for Zn^{2+} (as $ZnCl_2$) in immortalised HUVECs: (a) in the absence of FFAs with variable BSA concentration (0-0.6 mM); (b) with fixed extracellular BSA concentration (60 µM) in the presence or absence of fatty acids (FFAs): C8:0 octanoate, and C14:0 myristate. IC_{50} concentrations were determined in duplicate of triplicate experiments with cell viability determined using the Sulforhodamine B (SRB) assay.

Materials and Methods

Materials. Human umbilical vein endothelial cells (HUVECs) were immortalised using hTERT as described below and maintained in endothelial cell growth media (PromoCell GMBH, Germany). Earle's Balanced Salt Solution (EBSS; low $NaHCO_3$) was purchased from Lonza, UK. Cells were checked for mycoplasma-free status at 6-month intervals. Dulbecco's Modified Eagle Medium (DMEM), phosphate-buffered saline (PBS), Tris Base (pH 10, 1 mM) and Trypsin/EDTA solution (0.25%) were kindly prepared by technical services at the Department of Life Sciences (University of Warwick, UK). C-Chip Disposable hemocytometers were purchased from Labtech International. All other plastic products for cell culture were purchased from Greiner Bio-One (Gloucestershire, UK). Isotope-enriched ^{68}ZnO (>99%) was purchased from CK-Isotopes. Ultra-pure nitric acid (72% v/v) was freshly distilled before use. Milli-Q water (18.2 MΩ•cm at 298 K) was freshly purified by reverse osmosis before use. Acetonitrile (GC-MS grade), ammonium acetate (99.99% trace metals basis), ammonium hydroxide (28% NH_3; 99.99% trace metals basis), diisopropylethylamine, sulforhodamine B, zinc sulfate heptahydrate (99.995% trace metals basis), sodium octanoate, sodium myristate, sodium palmitate, bovine serum albumin (fatty acid-free) and all other reagents were purchased from Sigma Aldrich and used as received, unless indicated otherwise. Natural abundance Zn ICP-MS standard solution was purchased from Inorganic Ventures (CGZN1-1).

Immortalisation of primary human umbilical vein endothelial cells (HUVECs). Early passage primary HUVECs were obtained from TCS Cellworks (Buckinghamshire, UK) and grown in endothelial cell growth media containing supplement mix (complete media; PromoCell, Germany). HUVECs were grown to 70% confluency and transduced with supernatant from ψ-CRIPpBABEpurohTERT cells (as described in reference [1]) which were gifted by Prof. Andrew Riches (University of St Andrews). The ψ-CRIPpBABEpurohTERT cells were grown in DMEM supplemented with 2 mM glutamine and 10% foetal bovine serum (FBS) and reached confluency. The supernatant was collected, filtered (0.45 µm) and 10 µg mL^{-1} polybrene was added to enhance the binding of viral particles to the HUVEC membrane. Only a single transduction was performed. After 24 h, the supernatant was removed and HUVECs were given fresh complete medium. HUVECs were passaged and 0.2 µg mL^{-1} of puromycin was added to the medium for selection of cells.

Reverse transcription-polymerase chain reaction (RT-PCR). To establish the expression of endothelial markers (genes encoding CD32, von Willebrand factor and VE-cadherin) in the immortalised HUVECs, RNA was extracted using TRIzol reagent (Invitrogen, UK) according to the manufacturer's instructions. RNA was precipitated using isopropanol and quantified using by NanoVue (GE Healthcare, UK). A 2 µg aliquot of total RNA was reverse transcribed into cDNA using Oligo(dT)-15 primer (Promega, UK). One µL of the resultant cDNA sample was subjected to PCR analysis using Bio-X-ACT short mix (Bioline, UK) and 250 nM of each primer. The cycling profile was: 95°C for 30 s, 58°C for 30 s and 68°C for 30 s for 35 cycles, preceded

by a 2-minute enzyme activation at 95°C. Gene-specific primers for genes encoding CD31, vWF and VE-cadherin were designed and obtained from Eurofins Genomics (Ebersberg, Germany). PCR products were analysed on agarose gels composed of 1% (w/v) agarose, melted in Tris-acetate/EDTA-buffer (TAE-buffer). SyberSafe dye was added to the melted agarose to enable the detection of DNA in the gel. The gel was left to set and then was transferred into an electrophoresis tank containing TAE-buffer. Samples were prepared with a gel loading dye and Hyperladder I DNA-ladder was loaded (Bioline). Gels were run at 150 V for as long as required for the separation of bands. DNA was visualised in a Gel Doc XR+ Imager and analysed using Image Lab 2.0 software (Bio-Rad Laboratories, UK).

Preparation of isotope-enriched $^{68}Zn^{2+}$ stock solution. Isotope-enriched ^{68}ZnO was reacted with 2 molar equivalents of hydrochloric acid to obtain a solution of $^{68}ZnCl_2$. The pH of the stock solution was adjusted with HEPES buffer to achieve a final working pH = 7 and $[Zn^{2+}]$ = 0.5 mM in 1× HEPES-buffered EBSS. The isotopic abundance of the stock solution was measured by ICP-MS (Agilent 7900 series ICP-MS in helium collision gas mode) and abundances are reported in **Table S1**.

Preparation of sterile isotopic-enriched $^{68}Zn^{2+}$ solution for cell culture. The previously described preparation of 0.5 mM $^{68}Zn^{2+}$ stock solution in buffered EBSS was diluted with Milli-Q doubly deionized water to achieve a final working concentration of 40 µM. This solution was combined in equal volumes with a solution prepared in HEPES-buffered EBSS containing BSA (in each case at 2× final working concentration). The resultant solution was filtered using a 0.2 µm sterile filter and incubated at 310 K for 24 h. Final working concentrations: 20 µM $^{68}Zn^{2+}$, 1× BSA (as required; see **Table 1** and **ESI Tables S2-S15**).

Zinc uptake experiments. Briefly, 5 × 10^6 HUVECs were seeded in P145 dishes using Endothelial cell growth medium (PromoCell, Germany) and incubated until achieving >90% confluence. (310 K, 5% CO_2 humidified atmosphere). The supernatant medium was then removed by aspiration, and cells were treated with physiological concentrations of BSA (600 µM) and natural abundance Zn^{2+} (20 µM) prepared in HEPES-buffered EBSS for 24 hours (NB the growth of human umbilical vein endothelial cells is contact-inhibited). Cells were then washed thoroughly (3×) with PBS, and then treated with test solutions: isotope-enriched $^{68}Zn^{2+}$ (20 µM) with defined bovine serum albumin supplementation (0-600 µM). Cell pellets were collected in a time-dependent manner using 1 mL Trypsin/EDTA (0.25%) and were re-suspended in PBS to obtain a single cell solution, from which a cell count was obtained using a hemocytometer. Cell pellets were obtained by centrifugation and repeated washing with PBS (3 × 1 mL). Cells were then re-suspended in 200 µL ultra-pure 72% nitric acid and digested at 351 K. After 24 h, solutions were diluted with milli-Q water to achieve a final working nitric acid concentration of 3.6% v/v (4 mL). Zinc content (^{64}Zn, ^{66}Zn, ^{67}Zn, ^{68}Zn, ^{70}Zn) was determined using an Agilent 7900 series ICP-MS in He-gas mode. The instrument was calibrated using freshly prepared Zn standard solutions (0.1-1000 ppb) in 3.6% v/v nitric acid

with an internal standard of ^{166}Er (50 ppb). Data were processed using MassHunter (Agilent Technologies, Inc., UK). Each timepoint is the result of three biological repeats. For the experiments involving FFAs, isotope-enriched $^{68}Zn^{2+}$ (20 μM) media were prepared in the presence of 60 μM BSA with 5 mol. equiv. (300 μM) of FFAs, octanoate (C8:0), myristate (C14:0) or palmitate (C16:0), which were pre-incubated at 310 K for 24 h. Fatty acids were not co-administered in the pre-conditioning step of any experiment.

Determination of Zn^{2+} toxicity. Briefly, 5×10^4 HUVECs were seeded per well in a 96-well plate using 0.15 mL of endothelial cell growth medium per well and incubated for 48 h (310 K, 5% CO_2 atmosphere). After this time, the supernatant was removed and cells were treated with defined concentrations of Zn^{2+} (as $ZnCl_2$, typically 0.001-10 mM) in HEPES-buffered EBSS, in the absence of FFAs and in the presence of either 0, 6, 30, 60, or 600 μM BSA for 24 h. After this time, the supernatant was removed, and cells were washed with PBS (2×200 μL). Cells were then fixed by addition of 50% trichloroacetic acid (50 μL per well) and incubated at 277 K for 1 h. The supernatant was removed by sequential washing with water, and cells were stained using sulforhodamine B (0.4% dye content in 1% acetic acid solution) for 30 min. After this time, excess dye was removed by sequential washing with 1% acetic acid solution, and then dye was liberated by addition of Tris base (pH 10.5, 10 mM, 200 μL per well) for 1 h. Absorbance was measured using a Thermo Scientific SkanIt microplate reader fitted with a 492 nm filter. Absorbance measurements were normalized relative to untreated negative control wells to determine cell survival. IC_{50} value determinations were carried out as duplicate of triplicate experiments, and the IC_{50} values were calculated using Origin for Windows to fit sigmoidal curves to experimental data. Data are reported as the average of each duplicate experiment with associated standard deviation. The experiment was repeated with the following modification: Zn^{2+} toxicities were determined as described above using a fixed concentration of 60 μM bovine serum albumin (equivalent to 10% fetal calf serum routinely used in cell culture experiments) in the presence of FFA (0.3 mM, 5 mol. equiv., C8:0 octanoate or C14:0 myristate) for 24 h.

Calculation of free zinc concentrations. Free [Zn^{2+}] was estimated based on affinity data for the primary binding site, namely stoichiometric stability constants of log K = 7.0 and = 7.6.[2, 3] Using a published pK_a = 8.2,[2] these were converted to conditional stability constants valid at pH 7.4, giving log K' = 6.13 and 6.73. These were then used, together with total BSA and Zn^{2+} concentrations, to calculate free [Zn^{2+}], for both constants separately, to give an upper and lower limit. The data plotted in Figure 3(b) are the average of these two values. It may be noted that the resulting concentrations are likely an over-estimate, as they do not take binding to site B into account. We have refrained from attempting to include site B, as no stoichiometric or suitable conditional stability constant is available for this site.

Derivation of the Mathematical Model

Let $Q(t)$ denote the cellular zinc content (expressed in fg per cell). This zinc is present as various isotopes, denoted by a subscript $\star$, where $\star \in \{64,66,67,68,70\}$. These isotopes together constitute the total:

$$Q(t) = \sum_{\star \in \{64,66,67,68,70\}} Q_\star$$

The rate of change of $Q(t)$ is given by the difference between the influx φ_{in} and the efflux φ_{out}:

$$\frac{d}{dt}Q(t) = \varphi_{in} - \varphi_{out} .$$

We assume that fluxes are pro rata, that is $\varphi_{\star,in}(t) = r_{\star,ex}\varphi_{in}(t)$ where $r_{\star,ex} \in [0,1]$ is the relative abundance of isotope $\star$ in the extracellular medium, and similarly, $\varphi_{\star,out} = r_{\star,cell}\varphi_{out}$ where $r_{\star,cell} \in [0,1]$ is the relative abundance of isotope $\star$ inside the cells. We assume that $r_{\star,ex}$ remains constant for the duration of the experiment for all isotopes. This assumption is reasonable since the total extracellular quantity of zinc, circa 13 µg, exceeds the quantity contained in biomass by a factor of at least 30. By contrast, cellular abundances are changing over time as a result of influx (and efflux):

$$r_{\star,cell}(t) = \frac{Q_\star(t)}{Q(t)}$$

Furthermore, these changing cellular abundances are observed in the experiments which focus on the ratio $^{66}Zn/^{68}Zn$:

$$\frac{^{66}Zn}{^{68}Zn}(t) = \frac{r_{66,cell}}{r_{68,cell}}(t) = \frac{Q_{66}(t)/Q(t)}{Q_{68}(t)/Q(t)} = \frac{Q_{66}(t)}{Q_{68}(t)}$$

The pro rata assumption yields the kinetics for each isotope:

$$\frac{d}{dt}Q_\star(t) = \varphi_{\star,in}(t) - \varphi_{\star,out}(t) = r_{\star,ex}\varphi_{in}(t) - r_{\star,cell}(t)\varphi_{out}(t)$$

$$= r_{\star,ex}\varphi_{in}(t) - \frac{Q_\star(t)}{Q(t)}\varphi_{out}(t) .$$

Applying the quotient rule and substituting the above expressions for the rates of change of $Q(t)$ and $Q_\star(t)$, we find:

$$\frac{d}{dt}\frac{Q_\star(t)}{Q(t)} = \frac{\varphi_{in}(t)}{Q(t)}\left(r_{\star,ex} - \frac{Q_\star(t)}{Q(t)}\right) .$$

It is useful to switch to the auxiliary variable

$$W_\star(t) = r_{\star,ex} - Q_\star(t)/Q(t)$$

as this variable satisfies a particularly simple differential equation:

$$\frac{d}{dt}W_\star(t) = -\frac{\varphi_{in}(t)}{Q(t)}W_\star(t)$$

the solution of which is a standard formula:

$$W_\star(t) = W_\star(t_0)\exp\left\{-\int_{t_0}^{t}\frac{\varphi_{in}(\tau)}{Q(\tau)}d\tau\right\} .$$

This yields the following general solution for the observed isotope ratio:

$$\frac{^{66}\mathrm{Zn}}{^{68}\mathrm{Zn}}(t) = \frac{r_{66,ex} - W_{66}(t_0)G(t)}{r_{68,ex} - W_{68}(t_0)G(t)}$$

with

$$G(t) = \exp\left\{ -\int_{t_0}^{t} \frac{\varphi_{in}(\tau)}{Q(\tau)} d\tau \right\}.$$

The discussion to this point is valid even when the fluxes vary with time, but we now assume that they are constant over the duration of the experiment (*vide infra* for a justification of this assumption). We then have:

$$Q(t) = Q(t_0) + (\varphi_{in} - \varphi_{out})(t - t_0),$$

and with this, the integral in $G(t)$ can be evaluated to give:

$$G(t) = \left(1 + \frac{(\varphi_{in} - \varphi_{out})}{Q(t_0)}(t - t_0)\right)^{-\varphi_{in}/(\varphi_{in} - \varphi_{out})}.$$

In the special case where $\varphi_{in} = \varphi_{out} \equiv \varphi$ we have $Q(t) \equiv Q_0$, a condition we refer to as flux-balanced; in this case, $G(t)$ reduces to

$$G(t) = \exp\{-(\varphi/Q_0)(t - t_0)\}.$$

We now identify time $t = t_0$ as the start of the incubation experiment, and we assume that at this point in time, the cellular isotope abundances are equal to the natural ones, which we denote with a tilde. Recalling the definition of $W_\star$, we have:

$$\frac{^{66}\mathrm{Zn}}{^{68}\mathrm{Zn}}(t) = \frac{r_{66,ex} - (r_{66,ex} - \tilde{r}_{66})G(t)}{r_{68,ex} - (r_{68,ex} - \tilde{r}_{68})G(t)}.$$

The observed ratio thus shifts from $\tilde{r}_{66}/\tilde{r}_{68}$ at time t_0 to $r_{66,ex}/r_{68,ex}$ as $t \to \infty$.

Model selection and non-linear least-squares fitting. Prior to modelling the ^{66}Zn/^{68}Zn ratio data, linear regression was used to assess whether the cells accumulated a statistically significant amount of zinc during the experiment. If the null hypothesis of a slope equal to zero could not be rejected, the cells did not change their total content, meaning that flux-balance was given, and the equations valid for $\varphi_{in} = \varphi_{out} \equiv \varphi$ were used. The influx was estimated by non-linear least-squares fitting of the data to the model given above; for the flux-balanced case, Q_0 was set equal to 52 fg·cell^{-1}. If the null hypothesis was rejected, the parameters φ_{in} and φ_{out} were estimated by non-linear least-squares fitting of the ^{66}Zn/^{68}Zn data to the general model given above.

Non-linear least-squares curve fitting was carried out using `NonlinearModelFit` in Mathematica. A minimum was located, except in the [BSA] = 0 μM experiment, where the estimates for φ_{in} and φ_{out} converged to a common value in spite of clear evidence that $\varphi_{in} > \varphi_{out}$. To obtain a parameter estimate in this case, the quantity $(\varphi_{in} - \varphi_{out})$ was set equal to the estimated slope of the linear regression to the accumulation data, and only φ_{in} was subsequently estimated via the normal procedure.

Justification for assuming constant fluxes. To validate the assumption that fluxes were constant over time, an empirical reconstruction approach was used. Briefly, we have the following explicit expressions for the fluxes as a function of time:

$$\varphi_{in}(t) = -Q(t)\frac{G'(t)}{G(t)}$$

and

$$\varphi_{out}(t) = -Q(t)\frac{G'(t)}{G(t)} - Q'(t)$$

with

$$G(t) = \frac{r_{66,ex} - r_{68,ex}R(t)}{r_{66,ex} - {}_{66,ex} - (r_{68,ex} - \tilde{r}_{68,ex})R(t)}$$

where $R \equiv {}^{66}Zn/{}^{68}Zn$. This means that the fluxes can in fact be reconstructed as a function of time if R and Q have been sampled sufficiently frequently in time, with sufficient accuracy, to warrant the fitting of a suitable smooth curve. A drawback is that the expressions involve differentiation, which tends to exacerbate the effects of any inaccuracies. However, this approach was merely taken to test whether the assumption of time-constant influx and efflux over the course of the experiment was warranted. By way of representative example with relatively high influx and non-constant $Q(t)$, let us consider the accumulation and isotope ratio data for the [BSA] = 40 μM experiment. The figure below shows smooth curve fits to the data, giving $R(t)$ and $Q(t)$ empirically, as well as the resulting reconstructed fluxes. The latter are broadly consistent with the assumption of time-constant fluxes, although there is evidence that the efflux experiences a transient at the beginning of the experiment.

The assumption of constant fluxes is an idealisation that results in excellent goodness of fit, whereas the empirical-reconstructive approach suggests that the cells go through an initial period of acclimatisation. Inasmuch as the data do not clearly favour one or the other hypothesis, we have preferred to adhere to the simplicity of the mechanistic analysis presented in the main text.